Article

Nesprin-2G, a Component of the Nuclear LINC Complex, Is Subject to Myosin-Dependent Tension

Paul T. Arsenovic,[1] Iswarya Ramachandran,[1] Kranthidhar Bathula,[1] Ruijun Zhu,[2] Jiten D. Narang,[1] Natalie A. Noll,[1] Christopher A. Lemmon,[1] Gregg G. Gundersen,[2] and Daniel E. Conway[1,*]

[1]Department of Biomedical Engineering, Virginia Commonwealth University, Richmond, Virginia; and [2]Department of Pathology and Cell Biology, Columbia University, New York, New York

ABSTRACT The nucleus of a cell has long been considered to be subject to mechanical force. Despite the observation that mechanical forces affect nuclear geometry and movement, how forces are applied onto the nucleus is not well understood. The nuclear LINC (linker of nucleoskeleton and cytoskeleton) complex has been hypothesized to be the critical structure that mediates the transfer of mechanical forces from the cytoskeleton onto the nucleus. Previously used techniques for studying nuclear forces have been unable to resolve forces across individual proteins, making it difficult to clearly establish if the LINC complex experiences mechanical load. To directly measure forces across the LINC complex, we generated a fluorescence resonance energy transfer-based tension biosensor for nesprin-2G, a key structural protein in the LINC complex, which physically links this complex to the actin cytoskeleton. Using this sensor we show that nesprin-2G is subject to mechanical tension in adherent fibroblasts, with highest levels of force on the apical and equatorial planes of the nucleus. We also show that the forces across nesprin-2G are dependent on actomyosin contractility and cell elongation. Additionally, nesprin-2G tension is reduced in fibroblasts from Hutchinson-Gilford progeria syndrome patients. This report provides the first, to our knowledge, direct evidence that nesprin-2G, and by extension the LINC complex, is subject to mechanical force. We also present evidence that nesprin-2G localization to the nuclear membrane is altered under high-force conditions. Because forces across the LINC complex are altered by a variety of different conditions, mechanical forces across the LINC complex, as well as the nucleus in general, may represent an important mechanism for mediating mechanotransduction.

INTRODUCTION

The nucleus is typically the largest and perhaps the most critical organelle of a eukaryotic cell. The nucleus is directly connected to the cytoplasmic cytoskeleton by a class of nuclear membrane proteins known as nesprins that bind actin, intermediate filaments, and microtubules. Nesprins, together with SUNs and lamins, form the LINC (linker of nucleoskeleton to cytoskeleton) complex, physically linking the cytosolic cytoskeleton to the nuclear lamina. Mutations in LINC complex proteins are associated with a variety of human genetic diseases and are also observed in cancer (1). Thus, the linkage of the cytoskeleton to the nucleus appears to be essential to cell function and homeostasis, which may include transfer of forces from the cytoplasmic cytoskeleton onto the nucleus.

Evidence for mechanical forces at cell-matrix adhesions has existed for over 30 years (2). More recently mechanical forces have been measured across cell-cell adhesions (3,4). The model of cellular tensegrity predicts that cell-matrix and cell-cell forces are readily transferred across the cytoskeleton and applied to intracellular structures such as the nucleus (5). The tensegrity model is supported by experimental evidence showing mechanical force applied at the perimeter of the cell results in changes in nuclear shape (6–8). Nuclear forces have long been hypothesized to regulate cellular functions, including nuclear transport, DNA structure, and gene expression (9). Recently, Gabriele and colleagues (10,11) have inferred the forces on the nucleus by measuring nuclear deformation, but this approach assumes the actin cytoskeleton behaves as an elastic solid and the actin fibers can be approximated as two parallel fibers. In a more recent publication Lele and colleagues (12) showed that the nuclear position coincides with the point of maximum tension, suggesting that a protruding or retracting cell boundary transmits force onto the nucleus through the LINC complex.

Although there is significant evidence for the existence of nuclear forces, there is limited understanding of the specific proteins responsible for the transmission of force, largely due to a lack of techniques capable of measuring the forces applied to the load-bearing proteins that anchor the nucleus. Recently, a genetically encoded, calibrated fluorescence resonance energy transfer (FRET)-based tension biosensor was developed (13). This sensor consists of a linear-elastic spring between a FRET pair, and thus the FRET is inversely proportional to force. We and others have used the sensor to

Submitted February 18, 2015, and accepted for publication November 12, 2015.

*Correspondence: dconway@vcu.edu

Paul T. Arsenovic and Iswarya Ramachandran contributed equally to this work.

Editor: Catherine Royer.

0006-3495/16/01/0034/10

http://dx.doi.org/10.1016/j.bpj.2015.11.014

image mechanical tension across structural proteins in cell-cell (14–17) and cell-matrix (13) adhesions. Using the same FRET tension sensor module, we developed a mini-nesprin-2G tension sensor that directly measures mechanical tension applied to the LINC complex. Using this sensor we observed that mini-nesprin-2G (referred to as nesprin-2G hereafter) is subject to constitutive, actomyosin-dependent tension in resting fibroblasts. Changes in cell morphology altered nesprin-2G tension. Additionally, we observed reduced nesprin-2G tension in fibroblasts from Hutchinson-Gilford progeria syndrome (HGPS) patients. Our results provide the first, to our knowledge, direct evidence that nesprin-2G, a component of the LINC complex, is subject to significant mechanical force.

MATERIALS AND METHODS

Design of the nesprin tension sensor

The mouse mini-nesprin-2G tension sensor was designed based on the previous mini-nesprin-2G construct (18). GeneArt Gene Synthesis (Life Technologies, Carlsbad, CA) was used to chemically synthesize the mini-nesprin-2G linker, which consisted of the mini-nesprin-2G sequence, with an XhoI and NotI site linker between the 1-485 N-terminal actin binding CH region and the 6525–6874 C-terminal KASH (Klarsicht, ANC-1, Syne Homology) domain. A previously characterized FRET-based tension sensor (consisting of mTFP1 and venus separated by a 40 amino acid elastic linker, flanked by XhoI and NotI) (13), was inserted between the XhoI and NotI sites of the mini-nesprin-2G linker. The mini-nesprin-2G linker was then moved into pcDNA 3.1 (+) using *Hin*dIII and *Eco*RI sites. The headless mini-nesprin-2G linker was made by digesting the full-length tension sensor with XhoI and *Eco*RI (eliminating the 1-485 N-terminal domain) and inserting into pcDNA 3.1 (−) using the XhoI and *Eco*RI sites.

Cell culture

NIH3T3 mouse fibroblasts were cultured in Dulbecco's modified Eagle's medium (DMEM) with 10% fetal calf serum. Primary human fibroblasts were cultured in DMEM with 10% fetal bovine serum. Normal fibroblasts (catalog No. GM00316) and HGPS fibroblasts (catalog No. AG11498) were obtained from the Coriell Cell Repository (Camden, NJ). DNA plasmids were transfected into cells using Lipofectamine 2000 or 3000 (Life Technologies) per manufacturer instructions. In all experiments cells were allowed to adhere to fibronectin coated glass bottom dishes or coverslips overnight before imaging. In indicated experiments cells were treated with 1 nM calyculin A (Cell Signaling Technology, Danvers, MA) and imaged 5 to 20 min later. In other indicated experiments cells were treated simultaneously with 10 μM Y-27632 (R&D Systems, Minneapolis, MN) and 10 μM ML-7 (Sigma-Aldrich, St. Louis, MO) to reduce myosin activity and imaged 30 to 45 min later. Additional experiments were performed with Rho Activators I and II (Cytoskeleton, Denver, CO) per manufacturer instructions. To examine nuclear positioning and TAN (transmembrane actin-associated nuclear) lines, NIH3T3 fibroblasts were cultured in DMEM with 10% bovine calf serum (Hyclone, Logan UT) to confluent and starved for 48–72 h and the starved monolayer was wounded and then treated with 10 μM lysophosphatidic acid (LPA) for 2 h and 1 h, respectively, as previously described (19).

FRET image acquisition

Images were acquired from cells grown on glass bottom dishes on an inverted Zeiss LSM 710 confocal (Oberkochen, Germany) using a 458 nm excitation wavelength from an argon laser source. A plan-apochromat 63 × oil NA 1.4 objective lens was used for all images analyzed. Live cells expressing either soluble teal (mTFP1) or venus were imaged in spectral mode using a 32-channel spectral META detector to record the spectral fingerprints of each fluorescent protein. After acquisition of the spectral fingerprints, cells expressing the nesprin tension sensor were imaged using online-unmixing mode in the Zeiss Zen Software. Images were spectrally unmixed into teal and venus channels, respectively, during acquisition. In each experiment images were captured on the same day, with the gain and laser intensities fixed across all samples. During acquisition, images were captured in 16 bit mode and averaged 4 times.

FRET image analysis

First, all images were background subtracted in the teal and venus channels, respectively, to reduce noise. Second, all saturated pixels were removed. Ratio images were calculated by dividing the unmixed venus channel by the unmixed teal channel. To reduce FRET noise from edge artifacts, pixels with very large FRET ratios (>20) were removed from analysis. To examine FRET pixels of interest, ratio images were multiplied with binary image masks that outlined the nuclear membrane. Pixels from each experimental group were aggregated and sorted by their fluorescent intensity. To remove the influence of acceptor bleedthrough on the fret ratio, only intensity-sorted fret ratio pixels were compared across all experimental groups. Sorted pixels were binned into discrete intensity ranges and the average fret ratio in a given intensity range were compared, using an algorithm based on Chen et al (20).

Three-dimensional FRET analysis

On a per cell basis, z-stack confocal images were acquired as spectrally unmixed teal and venus images using Zeiss Zen software. In each cell z-stack, top, middle, and bottom image planes were extracted. For each image plane, binary masks were manually created in ImageJ to exclude pixels outside of the cell nucleus as determined by the transmission channel. Ratio FRET images were calculated by dividing unmixed venus images by unmixed teal images after background subtraction. The median of each ratio image was computed for each image plane (top, middle, and bottom). To determine the relative force distribution on a per cell basis, the FRET indices were normalized by the average of the medians for the top, middle, and bottom image planes of each cell.

Immunocytohistochemistry

Primary human fibroblasts or NIH3T3 cells were grown on fibronectin coated glass coverslips and fixed using 4% paraformaldehyde or methanol as indicated. Cells were permeabilized with 0.1% Triton X and stained with rabbit anti-nesprin-2G (19), mouse anti-vimentin (Santa Cruz, Santa Cruz, CA), or α-tubulin (Iowa Developmental Hybridoma Bank, gift of Amanda Dickinson), and detected by Alexa Fluor secondary antibodies (Life Technologies). Actin was labeled using rhodamine phalloidin (Cytoskeleton). Nuclei were counterstained using Hoechst 33342 (Life Technologies). Slides were mounted and images collected using a Zeiss 710 LSM confocal microscope.

shRNA and Western blotting

Short hairpin sequence and a detailed detection method for Nesprin-2G knockdown was described in Li et al., 2015 (21). Cells were directly lysed with 1X Laemmli sample buffer after phosphate buffered saline washout. Primary antibodies used to detect the signal are rabbit anti-nesprin-2G as described previously and mouse anti-GAPDH (clone 6C5, Life Technologies).

Micropatterning

Stamps of lines with varied widths: 5, 20, 40 μm and 1 cm in length were made with polydimethylsiloxane (PDMS). A coverslip was prepared with a thin layer of PDMS where it was to be stamped. The stamps were then coated with a layer of fibronectin and hand pressed onto the PDMS layer on the coverslip. The coverslips were rinsed and then treated with Pluronic F-127 solution to block cell adhesion to regions without fibronectin. Transfected cells were seeded onto the surface of the coverslip and cultured overnight before imaging. Unpatterned controls consisted of fibronectin that was directly pipetted onto a coverslip and allowed to adsorb.

Statistics

Sorted pixels, binned into discrete intensity ranges, were analyzed for statistical differences using *t*-test (for groups of two) or analysis of variance (ANOVA) with Newman-Keuls post-hoc test. Data were considered significant for p-values <0.05. Data on graphs are presented as mean $\pm$ standard error.

RESULTS

We sought to develop a biosensor to measure the mechanical forces applied across the LINC complex. Nesprin-1 and -2 are the principal isoforms that connect actin to the LINC complex, and we therefore hypothesized that a nesprin-2 biosensor could be used to measure actomyosin forces applied across the LINC complex. We designed a nesprin-2 FRET-based tension sensor (Fig. 1 *A*) based on a previously developed, artificially shortened form of nesprin-2G, known as mini-nesprin (18). Mini-nesprin-2G was previously shown to behave similar to endogenous nesprin-2G (including supporting actin-dependent nuclear movement) (18,19), supporting its suitability as an artificial sensor for measuring nesprin-2G forces.

When expressed in NIH3T3 mouse fibroblasts the nesprin tension sensor localized to the nuclear membrane (Fig. 1 *B*), similar to wild-type nesprin (see Fig. S4 in the Supporting Material and (18)). We also generated a headless control (Fig. 1 *A*) in which the actin-binding domain of nesprin was removed; this sensor also localized to the nuclear membrane. A major difference between the tension sensor and headless control was that only the tension sensor was organized into fibers in the cytoplasm (Fig. S1 *A*). This expression pattern is consistent with endogenous nesprin (see Fig. S4) and suggests that the ability to associate with actin is preserved in the nesprin tension sensor. Furthermore, we observed that actin was associated with the nuclear membrane in cells expressing the nesprin tension sensor, whereas actin localization to the nuclear envelope was reduced in cells expressing the headless control (see Fig. S1 *B*) further indicating that the nesprin-actin interaction is preserved in the biosensor. To determine if overexpression of the sensor induced a dominant negative KASH phenotype, in which nuclear-cytoskeletal connections are disrupted (22), we examined if expression of the tension sensor altered vimentin and α-tubulin morphology at the nucleus. Although we did not observe any significant morphological changes in vimentin or α-tubulin staining at the nucleus for cells expressing the nesprin-2G tension sensor as compared to untransfected cells (Fig. S1, *C* and *D*); nevertheless, high levels of expression of the nesprin-2G sensor may act like a dominant negative KASH, disrupting intermediate filament and microtubule interactions with the nuclear membrane. We also confirmed that the nesprin-2G tension sensor rescues centrosomal orientation and rearward nuclear movement in a wounded and LPA-stimulated monolayer of fibroblasts depleted of endogenous nesprin-2G, whereas overexpression of the headless control did not rescue the defect in the knockdown cells (Figs. 1 *D* and S2, *A–C*) (19). Furthermore, we observed that in these wounded, LPA-stimulated cells, the nesprin-2G tension sensor is associated with F-actin above the nucleus and colocalized with TAN lines and such colocalization is not present in the headless control. (Fig. S2, *D* and *E*) (19). Because the nesprin-2G tension sensor localizes to the nuclear membrane, interacts with actin, rescues nuclear movement, and incorporates into TAN lines, we conclude it retains similar biological function to endogenous nesprin-2G.

We examined FRET of the nesprin-2G tension sensor as compared to headless control. Initially, we limited our analysis to the equatorial plane in all samples (the plane where the diameter of the nuclear ring was the largest). In NIH3T3 cells the nesprin-2G tension sensor had significantly reduced FRET compared to the force-insensitive headless control (Fig. 1, *B* and *C*), indicating that the nesprin-2G sensor is subject to mechanical force. We also observed that the nesprin-2G sensor is subject to mechanical force in bovine aortic endothelial cells (D.E.C., unpublished data).

We then examined the distribution of force on the apical, equatorial, and basal planes of the nucleus. We observed that the FRET at apical and equatorial planes of the nucleus was significantly lower when compared to the basal plane on a paired cell basis (Fig. 1 *E*). There was no significant differences in FRET between the apical, equatorial, and basal planes on a paired cell basis when using the headless control (Fig. 1 *F*), suggesting that the tension sensor FRET differences are force mediated. Because each cell was individually background subtracted, FRET indices were normalized on a per cell basis. Thus, it is not possible to directly compare the FRET indices between tension sensor and headless in these experiments. Because the intensity of the sensor was greatest in the equatorial plane (resulting in a better signal/noise ratio), only the FRET at the equatorial plane was measured in the remainder of the experiments.

To assess the contribution of actomyosin contractility to nesprin-2G tension, we treated NIH3T3 fibroblasts with calyculin A. Calyculin A, inhibitor of protein phosphatase 1 and 2, results in increased myosin phosphorylation and contractility (23). The nesprin tension sensor in cells treated with calyculin A had significantly reduced FRET

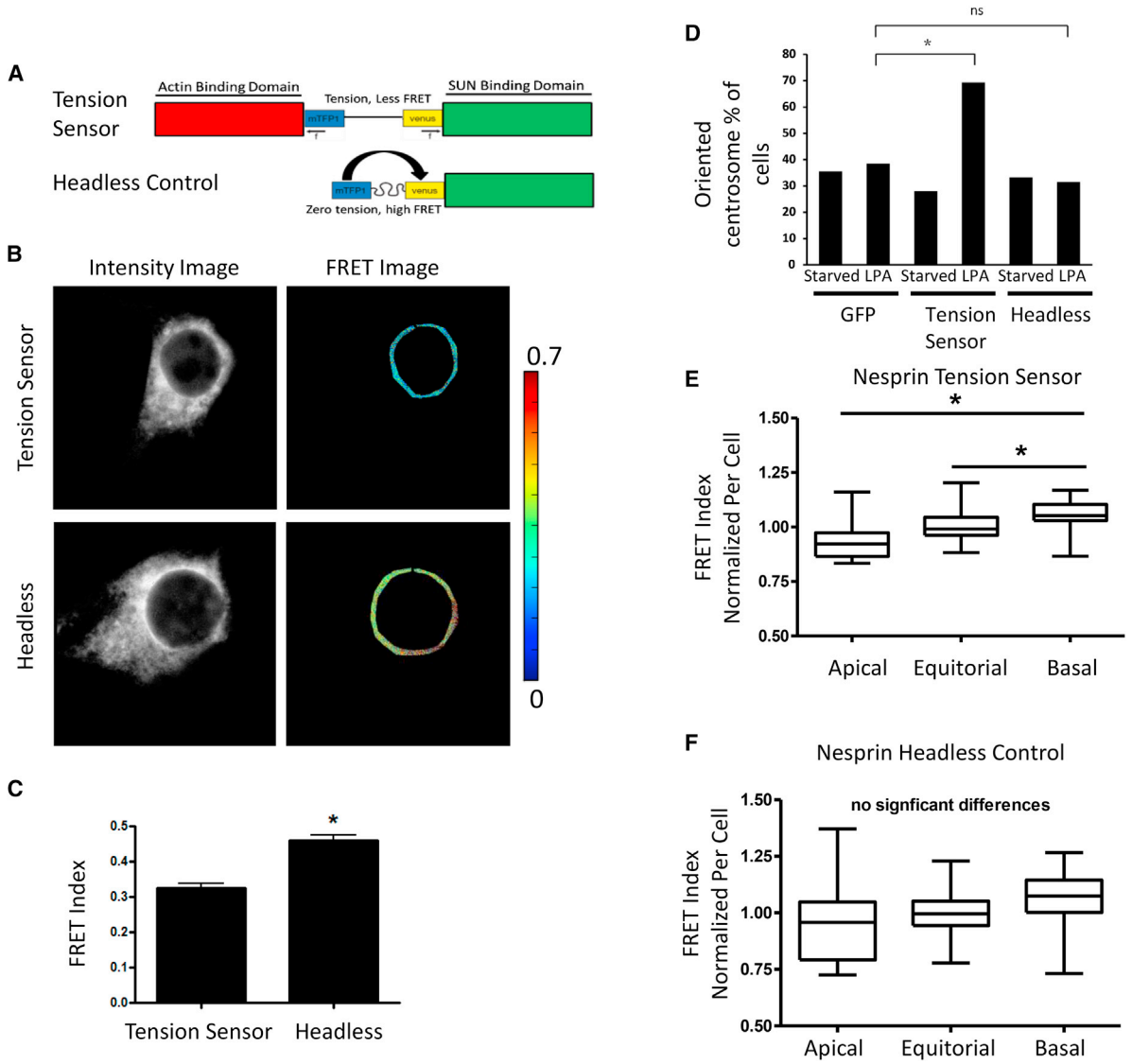

FIGURE 1 Nesprin tension biosensor. (*A*) Schematic of nesprin-2G tension sensor and headless control. (*B*) Nesprin-2G tension sensor and headless control localized to the nuclear membrane in NIH3T3 fibroblasts. The FRET at the nuclear envelope was reduced for the tension sensor as compared to the headless control. (*C*) The tension sensor had significantly reduced FRET at the nucleus as compared to the force-insensitive headless control, *t*-test, $p < 0.01$. Bar graphs represent FRET pixels from discrete intensity ranges collected across a minimum of 20 cells per condition. Similar results were obtained for three independent experiments. (*D*) Nesprin-2G tension sensor rescues centrosome orientation in nesprin-2G depleted cells subjected to scratch wounding and LPA treatment, Fisher's exact test, $*p < 0.05$; ns, not significant: $p > 0.05$. (*E*) The tension sensor relative FRET index per cell at various cross sections of the nucleus (*apical*, *equatorial*, and *basal*). Significantly reduced FRET was observed for apical and equatorial planes compared to basal (ANOVA, Newman–Keuls post-hoc test, $p < 0.01$). (*F*) No significant differences were observed for the headless control at various cross sections of the nucleus (*apical*, *equatorial*, and *basal*). To see this figure in color, go online.

as compared to untreated cells (Fig. 2, *A* and *B*). Treatment of cells with calpeptin, an indirect activator of Rho kinase (24), or a cell-permeable peptide that directly activates Rho kinase (25) also reduced FRET (Fig. S3, *A* and *B*). We also treated cells simultaneously with Y-27632 and ML-7, inhibitors of Rho (26) and myoslin light chain (27) kinases, respectively, to reduce myosin activity. The nesprin-2G tension sensor had higher FRET when myosin activity was inhibited as compared to untreated cells (Fig. 2, *A* and *B*). Blebbistatin, a more direct inhibitor of myosin activity, is autofluorescent and phototoxic at 458 nm excitation, therefore could not be used in combination with the tension sensor (28,29).

We then sought to understand how cell elongation affects force across nesprin-2G. To achieve uniform elongation, cells were grown on glass micropatterned with 20 μm wide lines of fibronectin or unpatterned fibronectin. We observed that cells grown on 20 μm lines had significantly decreased nesprin-2G FRET compared to cells grown on unpatterned surfaces (Fig. 3, *A* and *B*). We also observed

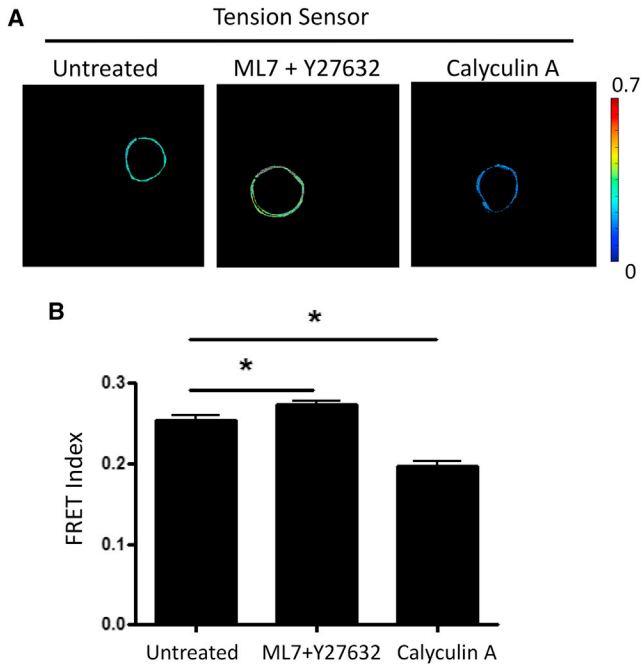

FIGURE 2 Role of myosin contractility on nesprin tension. (*A*) NIH3T3 cells expressing the nesprin tension sensor were treated with either 1 nM calyculin A or both 10 μM Y-27632 and 10 μM ML7 and were compared to unstimulated cells. (*B*) Statistical analysis of each condition showed that calyculin A treatment significantly reduced FRET, whereas Y27632 and ML7 treatment increased FRET, ANOVA Newman-Keuls post-hoc test, $p < 0.01$. Bar graphs represent FRET pixels from discrete intensity ranges collected across a minimum of 20 cells per condition. Similar results were obtained for two independent experiments. To see this figure in color, go online.

that 5 μm wide lines similarly decreased nesprin-2G FRET, whereas 40 μm lines did not (Fig. S5). In addition, we observed increased staining of endogenous nesprin-2G in cells on 20 μm lines (Fig. 3, *C* and *D*). Interestingly, nesprin-2G FRET ratios were homogeneous along the perimeter of the nucleus and were not significantly different at the regions with highest curvature (Fig. 3 *A*).

Finally, we sought to understand how nesprin-2G tension is affected by the disease HGPS, a rare genetic disorder in which young patients present clinically with premature aging. HGPS is caused by a mutation in lamin A that alters the splicing of the lamin A transcript, resulting in the loss of 50 amino acids of the protein and permanent farnesylation (30,31). Nuclei of HGPS patients, as well as normal cells expressing the lamin A truncation, have nuclei with altered morphology (blebbing) and altered mechanical stiffness (32). We examined nesprin-2G FRET in fibroblasts from an HGPS patient compared to a normal nondiseased patient. We observed increased nesprin-2G FRET in HGPS fibroblasts (Fig. 4, *A* and *B*). We did not observe significant differences in the fluorescent intensity of the nesprin-2G sensor at the nuclear envelope between HGPS and normal cells (Fig. 4 *C*). We also investigated if the localization of endogenous nesprin-2G at the nucleus was altered in HGPS cells. Although we did not observe any dramatic changes in nesprin localization in HGPS cells, when examined across multiple cells the intensity of nesprin-2G at the nuclear membrane was reduced relative to normal cells (Fig. S4, *A* and *B*).

DISCUSSION

Using a novel nesprin-2G FRET-based biosensor, we provide the first, to our knowledge, direct evidence of mechanical forces being applied across a nuclear membrane protein (Fig. 1). We also show that the force across nesprin-2G is sensitive to perturbations to actomyosin tension (Fig. 2), cell shape (Fig. 3), and a clinically relevant mutation in lamin A (Fig. 4). Because nesprin-2G has been shown to be one of several nesprin isoforms that serve as physical linkers between the LINC complex and the actin cytoskeleton (33), our data also indicate that the LINC complex, and by extension the nuclear membrane, are subject to mechanical loading, changing in response to a variety of biological conditions.

The existence of mechanical force on the nucleus is supported by a number of previous studies that have observed nuclear deformation in response to applied forces (6–8,22,34,35). Our tension sensor approach extends upon these prior finding by identifying a specific protein on the nuclear membrane subject to force. The finding of mechanical tension across nesprin-2G is in agreement with prior work that observed reduced nuclear deformation in cells with disrupted LINC complexes (22), impaired nuclear movement in cells depleted of nesprin-2G (19), as well as a recent report showing that nesprin-2 couples myosin force generation to nuclear translation (36).

Our approach to directly measure force with a protein-specific biosensor offers a number of advantages over previous methods to study nuclear forces. First, it allows for measurement of forces of cells in their native state, without the use of mechanical perturbations used by other nuclear force estimation methods. Second, our approach avoids the use of gene knockdowns and overexpression of dominant negative KASH proteins—it is possible that knocking down LINC proteins not only disrupts physical connections between the cytoskeleton and nucleus but also a host of intracellular signals. Third, the biosensor approach provides protein-specific resolution. Force biosensors can readily be developed for other nuclear proteins to map force transmission onto and within the nucleus. Finally, the sensor can be used to identify spatial differences in nesprin-2G force (Figs. 1 *E* and 3 *A*).

Because the FRET sensor is sensitive to the molecular conformation, our results are consistent with a model in which the FRET changes of the sensor can be interpreted to represent changes in the mechanical force across nesprin-2G. Changes in FRET could also be attributed to

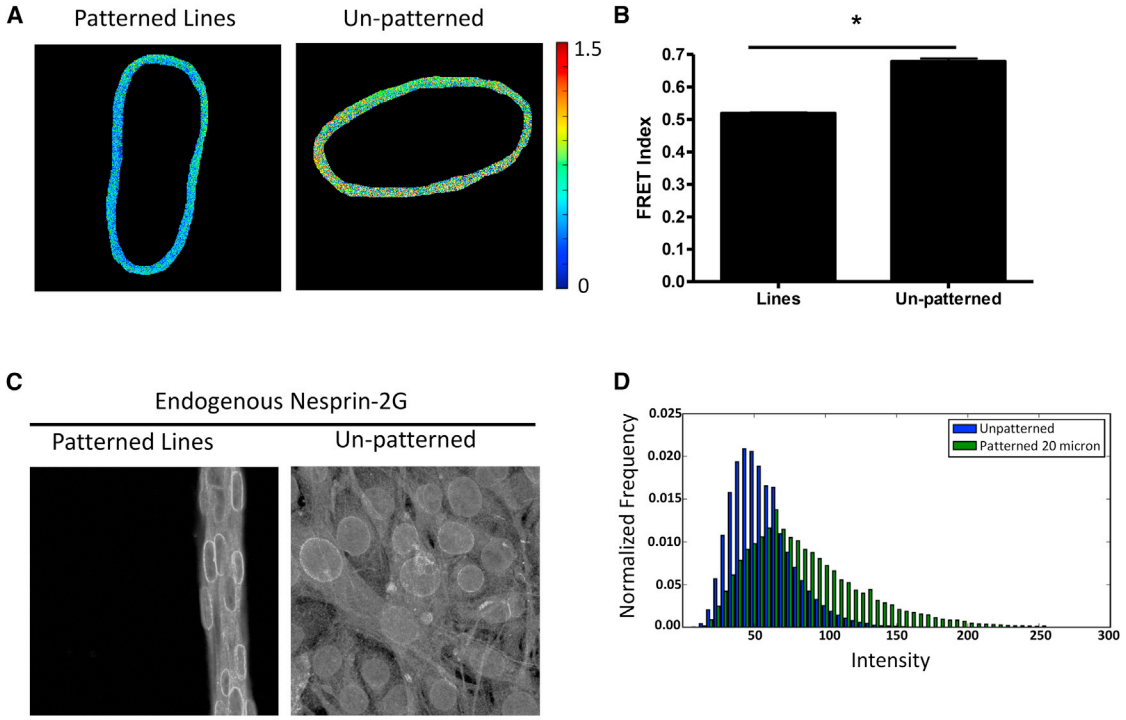

FIGURE 3 Effect of cell elongation on nesprin tension. (*A*) NIH3T3 cells expressing the nesprin tension sensor were grown overnight on 20 μm wide micropatterned lines of fibronectin or unpatterned fibronectin. (*B*) Statistical analysis of each condition showed that cells grown on lines had reduced FRET compared to cells grown on the unpatterned surface, *t*-test, $p < 0.01$. Bar graphs represent FRET pixels from discrete intensity ranges collected across a minimum of 15 cells per condition. Similar results were obtained for three independent experiments. (*C*) Untransfected cells grown on lines or unpatterned surfaces were fixed with paraformaldehyde and stained with nesprin-2 antibody. (*D*) Histogram analysis of nesprin-2 intensity at the nuclear membrane showed increased nuclear membrane nesprin-2 expression in cells on lines as compared to unpatterned surface (averaged across a minimum of four separate fields of view per condition). Histograms were normalized so that the area under each histogram sums to 1. To see this figure in color, go online.

changes in nesprin dimerization (creating intermolecular FRET (37)) or a loss of sensitivity due to overexpression of the sensor (resulting in a high background of zero force sensors). These different competing effects are not straightforward to parse. Although we cannot rule out changes in dimerization affecting FRET, we hypothesize that our "mini" nesprin-2G sensor has limited potential to dimerize because it lacks many of the spectrin repeats shown to promote nesprin oligomerization (38). We also sought to express the sensor at low expression levels to avoid loss of sensitivity. This is supported by histogram analysis of FRET, which indicated one discernible peak of FRET for each cell (Fig. S6). A significant unloaded FRET sensor population would likely result in a second peak on the FRET histogram. Furthermore, our experiments, which showed a relationship between FRET and actomyosin contractility, further support the FRET-force relationship of this sensor. We conclude that changes in FRET are the result of mechanical forces across nesprin-2G.

Nesprin-2G is believed to primarily interact with actin; therefore, our results likely reflect actin-mediated forces applied to the LINC complex. In addition to nesprin-2G, a number of other isoforms of nesprin-2 are expressed. Because some of these other isoforms lack either the actin binding domain or the SUN-binding KASH domain, they likely experience different levels of force or no force at all. In addition nesprin-1 is also connected to actin and may transfer actin-generated forces onto the LINC complex. Intermediate filaments and microtubules, which bind nesprin-3 and -4, respectively, could also contribute mechanical forces to the LINC complex. Intermediate filaments were shown to mediate nuclear positioning (39), nuclear volume (11), nuclear mechanical homeostasis (34), and nuclear movement during three-dimensional migration (40). Similarly designed nesprin-3 and -4 sensors would allow for measurement of intermediate filament and microtubule-based nuclear forces.

Our nesprin-2G sensor was designed based on the shortened mini-nesprin-2G, which lacks many of the spectrin repeats that promote nesprin oligomerization (38), as well as the kinesin binding domain (41). Gundersen and colleagues have shown that mini-nesprin-2G behaves similar to endogenous nesprin-2G, in that it is able to rescue TAN lines and nuclear movement in nesprin-2G depleted cells (18,19,42). This suggests that oligomerization and kinesin-binding are not essential for nuclear-cytoskeletal interactions, and our data further demonstrate that they are not required for force, at least in the cellular conditions tested here. The nesprin-2G

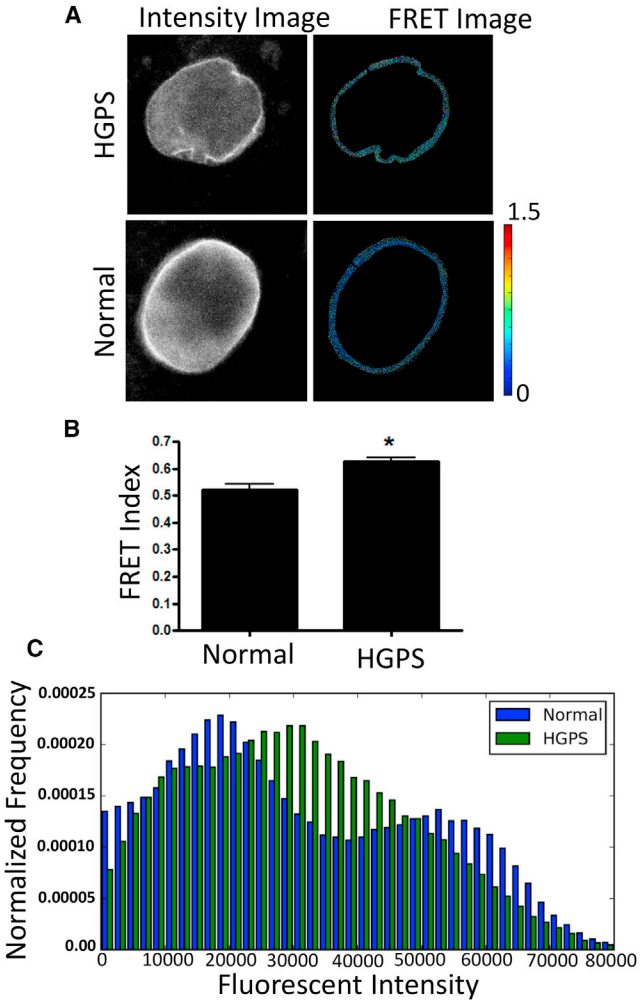

FIGURE 4 Nesprin tension in HGPS cells. (*A*) The nesprin tension sensor was expressed in normal and HGPS primary fibroblasts. (*B*) There was a significant increase in FRET for HGPS cells as compared to normal cells, *t*-test, $p < 0.01$. Bar graphs represent FRET pixels from discrete intensity ranges collected across a minimum of 20 cells per condition. Similar results were obtained for two independent experiments. (*C*) Histogram analysis of fluorescent intensity of the nesprin sensor for normal and HGPS cells. Histograms were normalized so that the area under each histogram sums to 1. To see this figure in color, go online.

sensor could be modified to incorporate the kinesin binding domain to assess the contribution of kinesin to force.

Our finding that nesprin-2G is subject to mechanical tension supports prior hypotheses that the LINC complex is similar to the load-bearing complexes at cell-cell and cell-matrix adhesions (33). A prior report showed that application of force to nesprin-1 of isolated nuclei generated a force-strengthening response (43), similar to the force-strengthening responses observed at cell-cell and cell-matrix adhesions. Our observation of higher nesprin-2G force and increased fluorescent intensity of endogenous nesprin-2G at the nuclear envelope in elongated cells (Fig. 3) may indicate that the LINC complex force-strengthens. Alternatively, it is possible that elongated cells have a higher density of nesprin molecules due to a reduction in nuclear volume. These results raise important questions as to how LINC complex assembly and response to force are regulated. Emerin phosphorylation has already been shown to regulate the LINC stiffening response (43); it will be interesting to determine if emerin regulates force across the LINC complex.

We also observed that although nesprin-2G force was increased in elongated cells, nesprin-2G forces remained isotropic (Fig. 3 *A*). Our data argue for a model in which nesprin-2G molecules are able to physically bend or rotate in the direction of applied force (Fig. 5, *A* and *B*), as proposed in (44). Alternatively, an increase in the recruitment of nesprin molecules to areas of high curvature could keep the force per nesprin molecule constant. Such a scenario would result in a homogenous FRET signal around the nucleus independent of the curvature as we observed (Fig. 3 *A*). However, the recruitment of nesprin to areas of high curvature would manifest in an uneven distribution of nesprin molecules around the nuclei of patterned cells. We did not observe an increase in nesprin intensity in elongated nuclei at the areas of highest curvature relative to regions of low curvature (Fig. 3 *C*). The latter observation is more consistent with the rotation of nesprin molecules as displayed in Fig. 5.

Interestingly, we observed the nesprin-2G FRET signal increased in cells patterned on 40 μm wide lines relative to unpatterned cells (Fig. S5). Although it is unclear why the tension on nesprin-2G would decrease on 40 μm relative to unpatterned cells, Khatau et. al. (45) observed the nuclear shape of mouse embryonic fibroblasts is more rounded on

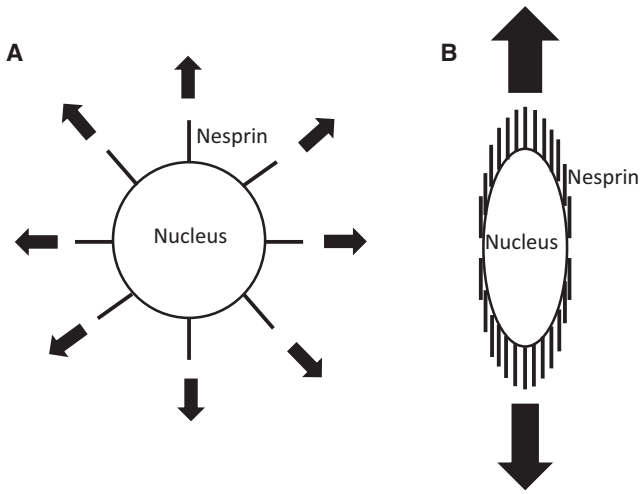

FIGURE 5 Model of nesprin-2 orientation in response to applied force. (*A*) Nesprin-2 is oriented radially for nonpolarized cells. (*B*) In elongated cells, in which actin stress fibers are oriented parallel to the longitudinal axis, there is more force applied to the LINC complex, as well as additional nesprin-2 molecules recruited to the nuclear membrane. Nesprin-2 forces are spatially homogenous around the periphery of the nucleus, suggesting that nesprin-2 orients in the longitudinal direction.

40 and 50 μm wide patterned lines relative to unpatterned controls. Although we did not quantify the aspect ratio of 3T3 fibroblast nuclei on patterned lines, nuclei of these cells may be similarly rounded on 40 and 50 μm lines. It is possible that the tension on nesprin-2G is a function of the nuclear shape, which is in turn driven by the focal adhesion geometry and cell-packing density.

Actin-generated compressive and tensile forces have been hypothesized to regulate nuclear shape (11,45,46). It was proposed that thick actin cables that surround the nucleus squeeze or compress vertically constrained nuclei into an elongated shape on patterned lines (11,45). Although it is possible compressive lateral forces mediate the elongation of patterned cell nuclei, our data showed high force on the lateral sides of the nucleus (Fig. 3, *A* and *B*). Therefore, we conclude that if actin is exerting compressive forces on the nucleus it is not through nesprin-2G. Although it is possible that lateral compressive forces are applied through other proteins besides nesprin-2G, recent work has shown that laser ablation of lateral stress fibers did not alter nuclear shape (12), suggesting that lateral forces are not necessary for nuclear shape. In addition, our observation of high tensile forces on the apical side of the nucleus (Fig. 1 *E*) does not support a model where apical actin primarily contributes compressive forces unless the compressive force is a result of the normal components of tension in the large actin fibers (45). Collectively, our data suggest that nesprin-2G at the apical surface of nuclei, as well as the lateral side of elongated nuclei, is subjected to a tensile-based shearing force (Figs. 1 *E* and 5 *B*). The nuclear surface, however, may still undergo compressive deformation, as compressive forces across other proteins may be larger than nesprin-2G forces. Thus, our data cannot establish the role of nuclear forces in mediating nuclear shape. The hypothesis that nuclear forces regulate nuclear shape has been questioned in a recent report by Dickinson and colleagues, which proposed that the shape of the nucleus is driven primarily by cell shape and not actomyosin-based forces on the nucleus (21). Even if nuclear forces do not regulate the shape of the nucleus, our data indicate that changes in nuclear shape are nonetheless associated with altered nuclear forces.

We have shown that nuclear forces are decreased in HGPS cells (Fig. 5, *A* and *B*). The reduction in force may be explained by a global reduction in actomyosin contractility, which is suggested from the observation that HGPS cells have reduced traction forces (47). Changes in LINC complex protein expression at the nuclear envelope have been reported for HGPS and other laminopathies (48,49). We also observed a decrease in the nuclear accumulation of nesprin-2G in HGPS cells (Fig. S4 *B*). Thus, changes in the distribution of other LINC proteins may also affect LINC complex forces. It is worth noting that the mechanical forces applied by the cytoskeleton onto the LINC complex may be independent of nuclear stiffness, which has been reported to be increased in HGPS cells (32). Future work will be important to determine if the decreased force on the LINC complex is causal for nuclear blebbing or advanced-aging symptoms in HGPS patients. It will be interesting to determine how farnesylation inhibitors (50) or the newly identified small molecule remodelin (51), both which have been shown to improve HGPS nuclear morphology, affect nuclear force.

We anticipate this newly developed biosensor will be an important tool to assess the role of nuclear forces in regulating cellular functions, providing answers to a number of long-held fundamental questions, most notably if changes in nesprin force can regulate gene expression or nuclear transport. Development of additional tension biosensors for other nuclear proteins that interact with lamin or DNA may be a useful tool to determine if nuclear forces are transmitted inside the nucleus, possibly onto chromosomal DNA. Because nearly every cell contains a nucleus, we anticipate the ability to measure forces on and within the nucleus will directly enhance the fundamental understanding of cellular biomechanics and mechanobiology, with wider application to the advancement of human health and disease.

SUPPORTING MATERIAL

Six figures are available at http://www.biophysj.org/biophysj/supplemental/S0006-3495(15)01171-6.

AUTHOR CONTRIBUTIONS

I.R. and D.E.C. designed the tension sensor; P.T.A., I.R., N.A.N., K.B., J.N., R.Z., and D.E.C. performed experiments; P.T.A., I.R., K.B., R.Z., C.A.L., G.G.G., and D.E.C. analyzed data; P.T.A. and D.E.C. wrote the article.

ACKNOWLEDGMENTS

We thank Tanmay Lele and Kris Dahl for helpful discussions and Amanda Dickinson for providing reagents.

This project was supported by start-up funding from the VCU School of Engineering (to D.E.C.), the Thomas F. and Kate Miller Jeffress Memorial Trust (to D.E.C.), and National Institutes of Health (NIH) grants GM 099481 (to G.G.G.) and GM115678 (to C.A.L.).

REFERENCES

1. Isermann, P., and J. Lammerding. 2013. Nuclear mechanics and mechanotransduction in health and disease. *Curr. Biol.* 23:R1113–R1121.
2. Harris, A. K., P. Wild, and D. Stopak. 1980. Silicone rubber substrata: a new wrinkle in the study of cell locomotion. *Science.* 208:177–179.
3. Liu, Z., N. J. Sniadecki, and C. S. Chen. 2010. Mechanical forces in endothelial cells during firm adhesion and early transmigration of human monocytes. *Cell. Mol. Bioeng.* 3:50–59.
4. Maruthamuthu, V., B. Sabass, …, M. L. Gardel. 2011. Cell-ECM traction force modulates endogenous tension at cell-cell contacts. *Proc. Natl. Acad. Sci. USA.* 108:4708–4713.
5. Ingber, D. E. 2003. Tensegrity I. Cell structure and hierarchical systems biology. *J. Cell Sci.* 116:1157–1173.

6. Maniotis, A. J., C. S. Chen, and D. E. Ingber. 1997. Demonstration of mechanical connections between integrins, cytoskeletal filaments, and nucleoplasm that stabilize nuclear structure. *Proc. Natl. Acad. Sci. USA.* 94:849–854.
7. Hu, S., L. Eberhard, …, N. Wang. 2004. Mechanical anisotropy of adherent cells probed by a three-dimensional magnetic twisting device. *Am. J. Physiol. Cell Physiol.* 287:C1184–C1191.
8. Hu, S., J. Chen, …, N. Wang. 2003. Intracellular stress tomography reveals stress focusing and structural anisotropy in cytoskeleton of living cells. *Am. J. Physiol. Cell Physiol.* 285:C1082–C1090.
9. Wang, N., J. D. Tytell, and D. E. Ingber. 2009. Mechanotransduction at a distance: mechanically coupling the extracellular matrix with the nucleus. *Nat. Rev. Mol. Cell Biol.* 10:75–82.
10. Versaevel, M., J.-B. Braquenier, …, S. Gabriele. 2014. Super-resolution microscopy reveals LINC complex recruitment at nuclear indentation sites. *Sci. Rep.* 4:7362.
11. Versaevel, M., T. Grevesse, and S. Gabriele. 2012. Spatial coordination between cell and nuclear shape within micropatterned endothelial cells. *Nat. Commun.* 3:671.
12. Alam, S. G., D. Lovett, …, T. P. Lele. 2015. The nucleus is an intracellular propagator of tensile forces in NIH 3T3 fibroblasts. *J. Cell Sci.* 128:1901–1911.
13. Grashoff, C., B. D. Hoffman, …, M. A. Schwartz. 2010. Measuring mechanical tension across vinculin reveals regulation of focal adhesion dynamics. *Nature.* 466:263–266.
14. Conway, D. E., M. T. Breckenridge, …, M. A. Schwartz. 2013. Fluid shear stress on endothelial cells modulates mechanical tension across VE-cadherin and PECAM-1. *Curr. Biol.* 23:1024–1030.
15. Kuriyama, S., E. Theveneau, …, R. Mayor. 2014. In vivo collective cell migration requires an LPAR2-dependent increase in tissue fluidity. *J. Cell Biol.* 206:113–127.
16. Borghi, N., M. Sorokina, …, A. R. Dunn. 2012. E-cadherin is under constitutive actomyosin-generated tension that is increased at cell-cell contacts upon externally applied stretch. *Proc. Natl. Acad. Sci. USA.* 109:12568–12573.
17. Cai, D., S.-C. Chen, …, D. J. Montell. 2014. Mechanical feedback through E-cadherin promotes direction sensing during collective cell migration. *Cell.* 157:1146–1159.
18. Ostlund, C., E. S. Folker, …, H. J. Worman. 2009. Dynamics and molecular interactions of linker of nucleoskeleton and cytoskeleton (LINC) complex proteins. *J. Cell Sci.* 122:4099–4108.
19. Luxton, G. W. G., E. R. Gomes, …, G. G. Gundersen. 2010. Linear arrays of nuclear envelope proteins harness retrograde actin flow for nuclear movement. *Science.* 329:956–959.
20. Chen, Y., J. P. Mauldin, …, A. Periasamy. 2007. Characterization of spectral FRET imaging microscopy for monitoring nuclear protein interactions. *J. Microsc.* 228:139–152.
21. Li, Y., D. Lovett, …, R. B. Dickinson. 2015. Moving cell boundaries drive nuclear shaping during cell spreading. *Biophys. J.* 109:670–686.
22. Lombardi, M. L., D. E. Jaalouk, …, J. Lammerding. 2011. The interaction between nesprins and sun proteins at the nuclear envelope is critical for force transmission between the nucleus and cytoskeleton. *J. Biol. Chem.* 286:26743–26753.
23. Chartier, L., L. L. Rankin, …, D. J. Hartshorne. 1991. Calyculin-A increases the level of protein phosphorylation and changes the shape of 3T3 fibroblasts. *Cell Motil. Cytoskeleton.* 18:26–40.
24. Schoenwaelder, S. M., and K. Burridge. 1999. Evidence for a calpeptin-sensitive protein-tyrosine phosphatase upstream of the small GTPase Rho. A novel role for the calpain inhibitor calpeptin in the inhibition of protein-tyrosine phosphatases. *J. Biol. Chem.* 274:14359–14367.
25. Schmidt, G., P. Sehr, …, K. Aktories. 1997. Gln 63 of Rho is deamidated by *Escherichia coli* cytotoxic necrotizing factor-1. *Nature.* 387:725–729.
26. Uehata, M., T. Ishizaki, …, S. Narumiya. 1997. Calcium sensitization of smooth muscle mediated by a Rho-associated protein kinase in hypertension. *Nature.* 389:990–994.
27. Saitoh, M., T. Ishikawa, …, H. Hidaka. 1987. Selective inhibition of catalytic activity of smooth muscle myosin light chain kinase. *J. Biol. Chem.* 262:7796–7801.
28. Kolega, J. 2004. Phototoxicity and photoinactivation of blebbistatin in UV and visible light. *Biochem. Biophys. Res. Commun.* 320:1020–1025.
29. Swift, L. M., H. Asfour, …, N. Sarvazyan. 2012. Properties of blebbistatin for cardiac optical mapping and other imaging applications. *Pflugers Arch.* 464:503–512.
30. Capell, B. C., M. R. Erdos, …, F. S. Collins. 2005. Inhibiting farnesylation of progerin prevents the characteristic nuclear blebbing of Hutchinson-Gilford progeria syndrome. *Proc. Natl. Acad. Sci. USA.* 102:12879–12884.
31. Goldman, R. D., D. K. Shumaker, …, F. S. Collins. 2004. Accumulation of mutant lamin A causes progressive changes in nuclear architecture in Hutchinson-Gilford progeria syndrome. *Proc. Natl. Acad. Sci. USA.* 101:8963–8968.
32. Verstraeten, V. L. R. M., J. Y. Ji, …, J. Lammerding. 2008. Increased mechanosensitivity and nuclear stiffness in Hutchinson-Gilford progeria cells: effects of farnesyltransferase inhibitors. *Aging Cell.* 7:383–393.
33. Alam, S., D. B. Lovett, …, T. P. Lele. 2014. Nuclear forces and cell mechanosensing. *Prog. Mol. Biol. Transl. Sci.* 126:205–215.
34. Neelam, S., T. J. Chancellor, …, T. P. Lele. 2015. Direct force probe reveals the mechanics of nuclear homeostasis in the mammalian cell. *Proc. Natl. Acad. Sci. USA.* 112:5720–5725.
35. Lovett, D. B., N. Shekhar, …, T. P. Lele. 2013. Modulation of nuclear shape by substrate rigidity. *Cell. Mol. Bioeng.* 6:230–238.
36. Thomas, D. G., A. Yenepalli, …, T. T. Egelhoff. 2015. Non-muscle myosin IIB is critical for nuclear translocation during 3D invasion. *J. Cell Biol.* 210:583–594.
37. LaCroix, A. S., K. E. Rothenberg, …, B. D. Hoffman. 2015. Construction, imaging, and analysis of FRET-based tension sensors in living cells. *Methods Cell Biol.* 125:161–186.
38. Taranum, S., I. Sur, …, A. A. Noegel. 2012. Cytoskeletal interactions at the nuclear envelope mediated by nesprins. *Int. J. Cell Biol.* 2012:736524.
39. Dupin, I., Y. Sakamoto, and S. Etienne-Manneville. 2011. Cytoplasmic intermediate filaments mediate actin-driven positioning of the nucleus. *J. Cell Sci.* 124:865–872.
40. Petrie, R. J., H. Koo, and K. M. Yamada. 2014. Generation of compartmentalized pressure by a nuclear piston governs cell motility in a 3D matrix. *Science.* 345:1062–1065.
41. Schneider, M., W. Lu, …, I. Karakesisoglou. 2011. Molecular mechanisms of centrosome and cytoskeleton anchorage at the nuclear envelope. *Cell. Mol. Life Sci.* 68:1593–1610.
42. Luxton, G. W. G., E. R. Gomes, …, G. G. Gundersen. 2011. TAN lines: a novel nuclear envelope structure involved in nuclear positioning. *Nucleus.* 2:173–181.
43. Guilluy, C., L. D. Osborne, …, K. Burridge. 2014. Isolated nuclei adapt to force and reveal a mechanotransduction pathway in the nucleus. *Nat. Cell Biol.* 16:376–381.
44. Lu, W., M. Schneider, …, I. Karakesisoglou. 2012. Nesprin interchain associations control nuclear size. *Cell. Mol. Life Sci.* 69:3493–3509.
45. Khatau, S. B., C. M. Hale, …, D. Wirtz. 2009. A perinuclear actin cap regulates nuclear shape. *Proc. Natl. Acad. Sci. USA.* 106:19017–19022.
46. Chancellor, T. J., J. Lee, …, T. Lele. 2010. Actomyosin tension exerted on the nucleus through nesprin-1 connections influences endothelial cell adhesion, migration, and cyclic strain-induced reorientation. *Biophys. J.* 99:115–123.
47. Booth-Gauthier, E. A., V. Du, …, B. Ladoux. 2013. Hutchinson-Gilford progeria syndrome alters nuclear shape and reduces cell motility in three dimensional model substrates. *Integr. Biol. (Camb).* 5:569–577.

48. Hale, C. M., A. L. Shrestha, …, D. Wirtz. 2008. Dysfunctional connections between the nucleus and the actin and microtubule networks in laminopathic models. *Biophys. J.* 95:5462–5475.

49. Chen, C.-Y., Y.-H. Chi, …, K.-T. Jeang. 2012. Accumulation of the inner nuclear envelope protein Sun1 is pathogenic in progeric and dystrophic laminopathies. *Cell.* 149:565–577.

50. Gordon, L. B., J. Massaro, …, M. W. Kieran; Progeria Clinical Trials Collaborative. 2014. Impact of farnesylation inhibitors on survival in Hutchinson-Gilford progeria syndrome. *Circulation.* 130:27–34.

51. Larrieu, D., S. Britton, …, S. P. Jackson. 2014. Chemical inhibition of NAT10 corrects defects of laminopathic cells. *Science.* 344:527–532.